Desalination 287 (2012) 350–361

Contents lists available at SciVerse ScienceDirect

Desalination

journal homepage: www.elsevier.com/locate/desal

Effects of process conditions in submerged ultrafiltration for refinery wastewater treatment: Optimization of operating process by response surface methodology

E. Yuliwati [a,b,c,1], A.F. Ismail [a,b,*], W.J. Lau [a,b], B.C. Ng [a,b], A. Mataram [a,b,d,2], M.A. Kassim [a,b]

[a] Advanced Membrane Technology Research Centre (AMTEC), Universiti Teknologi Malaysia, 81310 UTM Johor Bahru, Johor Darul Ta'zim, Malaysia
[b] Faculty of Petroleum and Renewable Energy Engineering, Universiti Teknologi Malaysia, 81310 UTM Johor Bahru, Johor Darul Ta'zim, Malaysia
[c] Faculty of Industrial Engineering, Universitas Bina Darma, 30251 Palembang, Indonesia
[d] Mechanical Engineering Department, Universitas Sriwijaya, Sumatera Selatan, Indonesia

ARTICLE INFO

Article history:
Received 7 June 2011
Received in revised form 30 July 2011
Accepted 23 August 2011
Available online 19 September 2011

Keywords:
Refinery wastewater
Submerged membrane
RSM
Air bubble flow rate
HRT

ABSTRACT

The influence of air bubble flow rate (ABFR), hydraulic retention time (HRT), mixed liquor suspended solid (MLSS) concentration, and pH on the performances of modified polyvinylidene fluoride (PVDF) was investigated in submerged membrane ultrafiltration (SMUF).The refinery wastewater process was conducted using an experimental set-up consisted of an SMUF reservoir, a circulation pump, and an aerator. For SMUF, operated at vacuum pressure, deposition and accumulation of suspended solids on membrane surface were prohibited with continuous aeration. The process performance was measured in terms of the membrane water flux and chemical oxygen demand (COD) removal efficiency. The air bubbles flow rate was controlled at 1.2–3.0 mL/min while HRT was manipulated in the range of 120–300 min. MLSS and pH solution were controlled at 4.5 g/L and 6.5, respectively. Results from response surface methodology (RSM) have demonstrated the improvement in water flux and COD removal, achieving 145.7 L/m^2 h and 90.8%, respectively. By using pH at 6.50, the optimized conditions achieved for refinery wastewater treatment were 2.25 mL/min, 276.93 min, 4.50 g/L for ABFR, HRT and MLSS concentration, respectively.

1. Introduction

The environment is becoming more polluted due to the various wastes discharged from a wide range of industrial applications. The economic growth in developing and developed countries has resulted in significant increase in production which in turn generates huge amount of undesirable wastes.The oil industry is one of the many industries which generate a vast amount of wastewater that is highly contaminated and difficult to treat. Several common techniques have been improved for removing soluble and insoluble organic and inorganic contaminants from refinery wastewater, such as gravity settling separation and mechanical coalescence, coagulation and air flotation, electrostatic and electrocoagulation separation. However, these methods would lead to a huge production of sludge and complicated operation problems [1]. Membrane technologies have greatly used in separation facilities to separate liquid/liquid or liquid/solid mixtures due to the suitable pore sizes and capability of removing emulsified oil droplets and other organic contaminants [2,3]. Ultrafiltration has been demonstrated as an efficient method in wastewater treatment, especially submerged membrane ultrafiltration that has been successfully applied to the refinery wastewater treatment. Thus, a stricter discharge standard is required in order to ensure the wastewater discharged is safe to the environments. For instance, in Malaysia, the effluent discharged from industrial sectors should comply with the national primary regulatory of discharged standard — Standard B [4].

Table 1 shows the characteristics of typical refinery wastewater together with the discharged standard set by Malaysian government. As can be clearly seen, it is compulsory to have a treatment plant in oil industry in order to comply with the environmental regulations. Technologies that can treat large quantities of wastewater with relatively small requirements are, therefore, of particular importance. The developed submerged membrane technology is proven to be able to completely retain biomass and operate at high suspended solids concentration with a relatively small footprint compared to other technologies.

The submerged hollow fiber membrane is now widely used in water and wastewater treatments due to its high packing density and ease of module manufacture and operation [5–7]. The removal of organic wastes from wastewater is, therefore, becoming increasingly important, and submerged ultrafiltration finds its application in this area. The direct immersion of hollow fiber membranes was assembled in the feed reservoir with withdrawal of liquid through the fibers by the application of a vacuum on the outlet of the fiber lumen [8–13]. Organic material is usually transformed to oils, solids, and gas, in that order. Gas can burn to provide energy to the system

* Corresponding author at: Advanced Membrane Technology Research Centre (AMTEC), Malaysia. Tel.: +60 7 553 5592; fax: +60 7 558 1463.
E-mail address: afauzi@utm.my (A.F. Ismail).
[1] Tel.: +62 711 515 679; fax: +62 711 518 000.
[2] Tel.: +62 711 580272.

0011-9164/$ – see front matter © 2011 Elsevier B.V. All rights reserved.
doi:10.1016/j.desal.2011.08.051

Table 1
Composition of synthetic refinery wastewater and the national discharge standards for refinery wastewater.

Constituent, unit	Concentration	Standard B
pH	6.7	5.5–9.0
Oil and grease, mg/L	17.0[a](±1.02)	10.0
COD, mg/L	555.0 (±0.25)	100
NH_3-N, mg/L	29.1 (±1.02)	20.0
Suspended solid, mg/L	213.0 (±0.07)	100.0
Chlorine free, mg/L	4.6 (±2.01)	2.0
Sulfide, mg/L	2.5 (±0.54)	0.5

[a]The numbers shown in parenthesis are standard deviation.

and oil can be better upgraded to enhance the value of some components. There has been increasing attention to the application of refinery effluent in petroleum industry over the last few years because refinery wastewaters are characterized by presence of several aromatic hydrocarbons and inorganic substances such as, chemical oxygen demand (COD), total organic carbon (TOC), sulfide, ammonia nitrogen (NH_3-N), and total suspended solid (TSS) [14–18].

As reported in most of the articles, SMUF has been conducted using one process variable at a time approach, i.e. the influence of variables is investigated separately. Using this approach, one requires conducting a large amount of experiments before a conclusion on the process performance could be drawn. The use of statistical methods such as response surface methodology (RSM) therefore could overcome the limitations of the one-variable at a time approach [19–25]. It is generally agreed that RSM is an efficient statistical tool, which can be used for modeling and optimization of several process variables [26]. Using developed response surface plots, one could understand better the relationship between factors (process variables) and responses (outcomes of experiments).

The main objective of this study is to investigate the effects of four different process variables, i.e. ABFR, HRT, MLSS and pH on the performances of modified PVDF membranes based on the approach of RSM (Design expert® 8.0.5.2). The experimental runs were designed in accordance with the central composite design and carried out batchwise. All the refinery wastewater used in this study was synthesizedly prepared based on ASTM D-1141-90.

2. Experimental

2.1. Synthetic refinery wastewater

The refinery wastewater which was prepared and used as feed solution in submerged ultrafiltration experiments was very similar to the characteristics of typical refinery wastewater shown in Table 1 [27].

Table 2
Properties of modified PVDF ultrafiltration membrane.

Parameter	Membrane
Membrane configuration	Hollow fiber
Membrane material	PVDF
Hydrophilic additive added	LiCl
Outer diameter (mm)	1.1
Inner diameter (mm)	0.55
Pore size (nm)	34.05
Contact angle (°)	54
Zeta potential (mV at pH 6.9)	62
Tensile strength (M Pa)	3.37 ± 0.13
Young's modulus (G Pa)	3.81 ± 0.21
Pure water flux ($L\,m^{-2}\,h^{-1}$)	82.95 at 250 mm Hg

2.2. Submerged ultrafiltration membrane

The experimental set-up shown in Fig. 1 has been used in this work. It was comprised of two main parts: the pretreatment tank and the membrane separation unit equipped with a fiber glass tank. The membrane separation unit was consisted of a reservoir of 14 L in volume, two hollow fiber bundles, a peristaltic pump, permeate flowmeter, and an effluent tank.

Table 2 shows the properties of PVDF membranes used in this experiment. In order to enhance membrane hydrophilicity of PVDF membranes, LiCl and TiO_2 were added to the spinning dope during membrane preparation process with the effort to improve membrane water productivity. The porous structure and possible hydrophilicity of the TiO_2 nanoparticles were directly correlated with porosity and might be responsible for the higher liquid uptake. As can also be seen in Fig. 2, the membranes used to treat refinery wastewater demonstrated a microporous surface which is in good agreement with the properties of ultrafiltration. The details of the membrane fabrication process and its properties on determination procedure could be found elsewhere [28].

The filtration experiments were carried out in vacuum. The liquid level in the feed tank was maintained constant throughout experiment. The air scouring bubble generated was advantageous to exert shear stress to minimize particles deposited on the membrane surface during filtration process.

Fig. 3 illustrates the flow pattern of air bubble within the submerged UF system. Two bundles of modified PVDF hollow fibers with total effective area of approximately 184 cm^2 were immersed

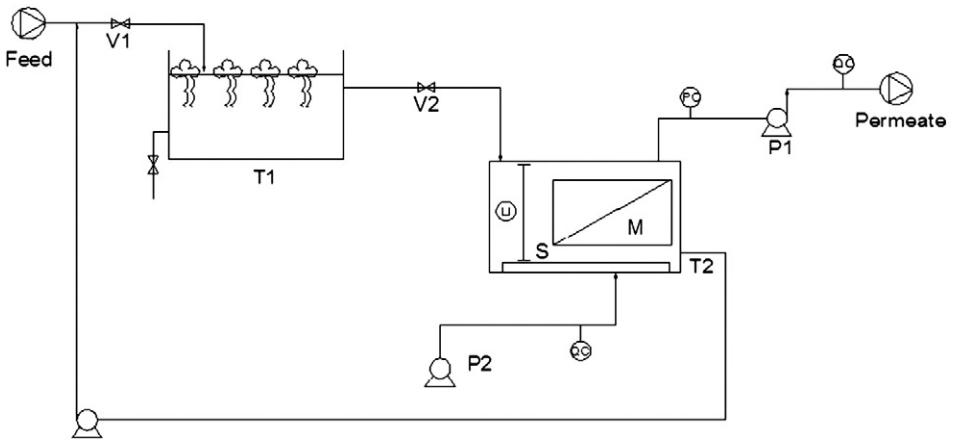

Fig. 1. Scheme of the submerged membrane system (V_1: wastewater valve, T_1: biological treatment tank, V_2: feed membrane reservoir valve, S: sparger, M: membrane module, T_2: membrane reservoir, P_1: peristaltic pump, P_2: air pump, QC: flow control, LC: liquid control, LI: level indicator, PC: pressure control).

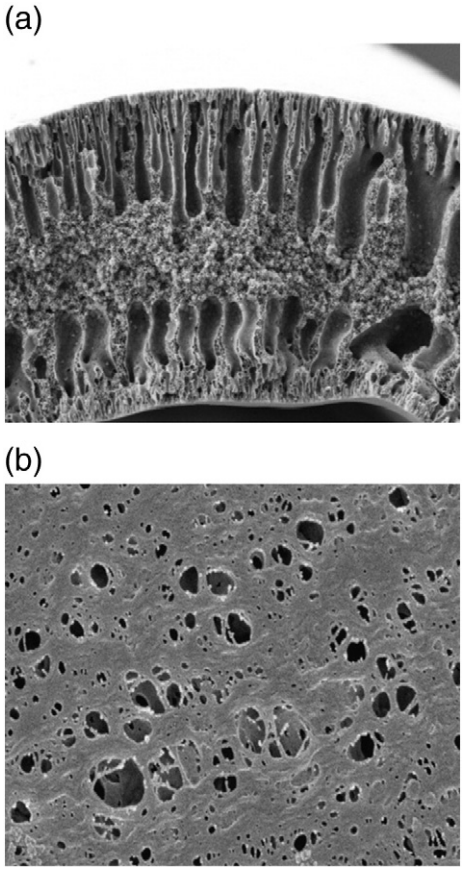

Fig. 2. FESEM images of the (a) cross section (Mag. 500×) and (b) outer surface (Mag. 40.0 k×) of modified PVDF membrane.

in the membrane reservoir and a constant TMP was maintained to pressurize wastewater from outside to inside of hollow fibers. All filtrations were conducted at room temperature and vacuum condition created using a peristaltic pump (Master flex model 7553-79, Cole Palmer). The permeate flow rate was continually recorded using flowmeter. The volume of the water permeation collected was determined using a graduated cylinder. After completing the filtration, the membrane surface was cleaned with a soft sponge to remove the particle-packed layer which might form during filtration.

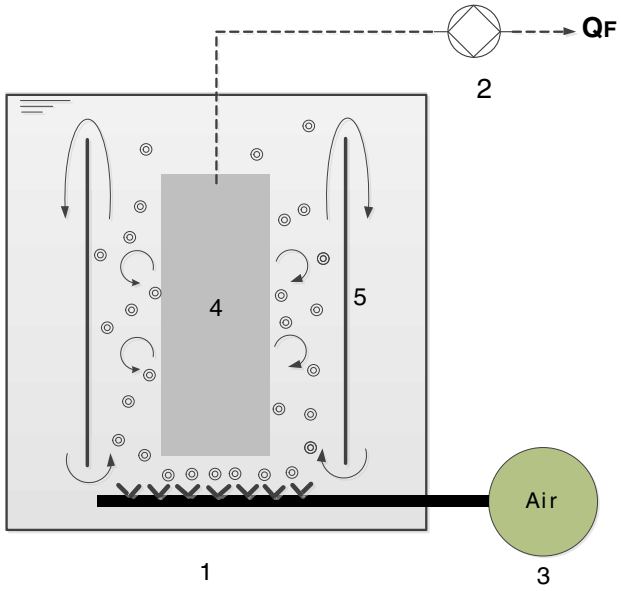

Fig. 3. Schematic representation of the air bubble up flow stream in submerged hollow fiber UF system: membrane reservoir (1); peristaltic pump (2); aerator (3); membrane bundles (4) and partitioned glass (5).

2.3. Analytical methods

Field emission scanning electron microscope (JEOL JSM-6700F) was used to examine the morphology of the PVDF hollow fiber membrane prepared. Prior to analysis, the membrane samples were first immersed in liquid nitrogen and fractured carefully. The samples were then coated with sputtering platinum before testing. The FESEM micrographs of cross-section and outer surface of the hollow fiber membranes were taken at various magnifications.

Tensile testing was performed at room temperature on a tensile tester LRX2 SKN LLYOD instrument. Tests were conducted on a cross head speed at 20 mm min^{-1} at break and gate length of filament at 25 mm [29,30]. At least five measurements were performed for each membrane sample, and the average values are reported in this study.

Membrane was tested with a self-made U-shape membrane bundle. Pure water permeation rate was measured after the steady state was reached, using the following equation:

$$F = \frac{V}{At} \tag{1}$$

where F is the pure water flux (L/m^2 h), V is the permeate volume (L), A is the membrane surface area (m^2), and t is the time (h).

COD concentrations were measured using a spectrophotometer (DR5000, HACH, Method 8000, TNT822, 20-1500 mg/L COD) in accordance to the standard procedures. During the operation with high organic loading rates, the parameters were evaluated daily and sampling was carried out three times a week again. The COD removal efficiencies are calculated with Eq. (2):

$$\text{COD removal } (\%) = \frac{COD_0 - COD}{COD_0} \times 100 \tag{2}$$

where COD_0 and COD are the initial concentration of synthetic refinery wastewater and the concentration of permeate produced.

2.4. Experimental design and optimization

RSM is derived from mathematical and statistical technique. It can be used for studying the effect of several factors at different level and their influence on each other. RSM has 4 major steps, which are experimental design, model fitting, model validation and condition optimization. Experimental designs such as Central Composite Designs (CCD) are useful for RSM. It does not require an excessive number of experimental runs. Based on the CCD of RSM with a total of 28 experiments, the four factors made up of ABFR, HRT, MLSS, and pH were used in this study. The designs

Table 3
Independent variables and limit level for response surface study.

Variables	Unit	Symbols		Levels				
		Coded	Uncoded	−2	−1	0	+1	+2
Air bubble flow rate	mL/min	x_1	X_1	0.3	1.2	2.1	3.0	3.9
HRT	min	x_2	X_2	120	180	240	300	360
MLSS	mg/L	x_3	X_3	1.5	3.0	4.5	6.0	7.5
pH	pH	x_4	X_4	3.5	5.0	6.5	8.0	9.5

Note: $\alpha = 2$.

Table 4
Experimental layout designed by Design-Expert and its corresponding experimental and predicted values of responses.

Standard	Factor variables				Responses			
	ABFR, mL/min	HRT, min	MLSS g/L	pH	Flux, L/m^2 h		COD retention, %	
					Experimental	Predicted	Experimental	Predicted
1	1.20	300.00	3.00	5.00	140.09	140.10	61.16	61.27
2	3.00	300.00	3.00	5.00	147.02	147.01	63.52	63.44
3	1.20	180.00	6.00	5.00	138.36	138.36	65.34	65.44
4	3.00	180.00	6.00	5.00	142.78	142.79	66.79	66.70
5	1.20	300.00	6.00	5.00	46.31	46.29	81.73	81.82
6	3.00	300.00	6.00	5.00	87.75	87.74	81.64	81.54
7	1.20	180.00	3.00	8.00	53.59	53.60	81.92	82.00
8	3.00	180.00	3.00	8.00	85.81	85.80	84.18	84.07
9	1.20	300.00	3.00	8.00	61.81	61.83	72.14	72.25
10	3.00	300.00	3.00	8.00	81.63	81.67	72.70	72.62
11	1.20	180.00	6.00	8.00	81.52	81.53	74.23	74.34
12	3.00	180.00	6.00	8.00	92.74	92.77	75.07	74.89
13	1.20	300.00	6.00	8.00	44.05	44.07	89.56	89.65
14	3.00	300.00	6.00	8.00	57.07	57.05	90.91	90.80
15	1.20	240.00	4.50	6.50	61.38	61.37	88.55	88.64
16	3.00	240.00	4.50	6.50	58.95	58.97	88.72	88.62
17	0.30	120.00	4.50	6.50	108.59	108.60	89.67	89.30
18	3.90	360.00	4.50	6.50	106.09	106.10	90.76	91.14
19	2.10	240.00	1.50	6.50	87.41	87.41	86.52	86.52
20	2.10	240.00	7.50	6.50	140.81	140.82	89.67	89.67
21	2.10	240.00	4.50	3.50	174.91	174.91	59.38	59.34
22	2.10	240.00	4.50	9.50	37.97	37.97	93.33	93.37
23	2.10	240.00	4.50	6.50	219.93	219.93	77.57	77.57
24	2.10	240.00	4.50	6.50	41.87	41.87	78.68	78.68
25	2.10	240.00	4.50	6.50	141.37	140.10	90.02	89.95
26	2.10	240.00	4.50	6.50	140.53	140.10	89.24	89.95
27	2.10	300.00	3.00	5.00	138.40	140.10	90.00	89.95
28	2.10	300.00	3.00	5.00	140.10	140.10	90.54	89.95

Table 5
ANOVA for response surface reduced quartic model (partial sum of squares — type III) response: flux.

Source	Sum of squares	Degree of freedom	Mean square	F-value	Prob>F
Model	58,310.22	23	2535.23	2157.23	<0.0001[a]
A	3.13	1	3.13	2.66	0.1781
B	1426.18	1	1426.18	1213.87	<0.0001
C	9376.34	1	9376.34	7980.50	<0.0001
D	15,852.18	1	15,852.18	13,492.29	<0.0001
AB	79.76	1	79.76	67.89	0.0012
AC	109.28	1	109.28	93.01	0.0006
AD	117.40	1	117.40	99.92	0.0006
BC	0.003489	1	0.003489	0.002969	0.9592
BC	160.23	1	160.23	136.38	0.0003
CD	2462.51	1	2462.51	2095.92	<0.0001
A^2	1430.17	1	1430.17	1217.26	<0.0001
B^2	900.31	1	900.31	766.28	<0.0001
C^2	1510.48	1	1510.48	1285.61	<0.0001
D^2	112.85	1	112.85	96.05	0.0006
ABC	11.48	1	11.48	9.77	0.0353
ABD	9.40	1	9.40	8.00	0.0474
ACD	428.57	1	428.57	364.77	<0.0001
BCD	32.78	1	32.78	27.90	0.0062
A^2B	561.72	1	561.72	478.09	<0.0001
A^2C	510.90	1	510.90	434.84	<0.0001
A^2D	3498.59	1	3498.59	2977.76	<0.0001
AB^2	389.17	1	389.17	331.24	<0.0001
A^2B^2	4299.18	1	4299.18	3659.17	<0.0001
Residual	4.70	4	1.17		
Lack of fit	0.000929	1	0.000929	0.000593	0.9821[b]
Pure error	4.70	3	1.57		
Cor total	58,314.92	27			
Std. dev.	1.08		R^2		0.9999
Mean	102.11		Adjusted R^2		0.9995

Values of 'Prob>F' less than 0.0500 indicate model terms are significant.
[a] Significant.
[b] Not significant.

Table 6
Anova for response surface reduced quartic model (partial sum of squares — type III) response: COD removal.

Source	Sum of squares	Df	Mean square	F-value	Prob>F
Model	2906.85	22	132.13	508.75	<0.0001[a]
A	5.10	1	5.10	19.63	0.0068
B	4.97	1	4.97	19.13	0.0072
C	1736.74	1	1736.74	6687.20	<0.0001
D	0.61	1	0.61	2.36	0.1848
AB	0.019	1	0.019	0.071	0.7999
AC	0.14	1	0.14	0.56	0.4892
AD	0.59	1	0.59	2.27	0.1922
BC	9.57	1	9.57	36.86	0.0018
BC	4.96	1	4.96	19.08	0.0072
CD	5.15	1	5.15	19.82	0.0067
A^2	0.095	1	0.095	0.37	0.5715
B^2	4.58	1	4.58	17.62	0.0085
C^2	246.43	1	246.43	948.84	<0.0001
D^2	186.53	1	186.53	718.21	<0.0001
ABC	0.20	1	0.20	0.78	0.4170
ABD	0.34	1	0.34	1.32	0.3020
ACD	0.19	1	0.19	0.75	0.4260
BCD	0.54	1	0.54	2.07	0.2093
A^2B	0.029	1	0.029	0.11	0.7502
A^2D	77.99	1	77.99	300.28	<0.0001
ABCD	1.39	1	1.39	5.35	0.0686
A^2B^2	180.18	1	180.18	693.78	<0.0001
Residual	1.30	5	0.26		
Lack of fit	0.43	2	0.22	0.75	0.5435[b]
Pure error	0.86	3	0.29		
Cor total	2908.15	27			
Std. dev.	0.51		R^2		0.9996
Mean	80.84		Adjusted R^2		0.9976

Values of 'Prob>F' less than 0.0500 indicate model terms are significant.
[a] Significant.
[b] Not significant.

were based on two-level full factorial design, which was augmented with center and star points. The total number of experiments of the design (N) can be calculated as follows,

$$N = N_a + N_o + N_c \tag{3}$$

where N_a is the number of the experiments of the two level full factorial design, N_o is the number of center points, and N_c is the number of star points.

Model fitting to equation of up to the fourth-order polynomial was performed to determine the goodness-of-fit. The responses were fitted to the variables by multiple regression. The minimum and maximum range of variables was investigated and the full experimental plan with respect to their values in actual and coded form was listed in Table 3. The actual and predicted values of the four independent variables together with the responses are summarized in Table 4.

The principle of RSM was described by Khuri and Cornell [31]. It is very important to choose an appropriate model for describing the shape of the surface well. To identify the right model that can fit the data, it can be started with the simplest model forms like first- and second-degree Scheffe's polynomial. After testing these models for adequacy of fit, they were augmented to simplex centroid and special quartic models by adding the appropriate terms. In this study, the quartic model used for predicting the optimal point was according to Eq. (4) as follows:

$$y = a_0 + a_1x + a_2x^2 + a_3x^3 + a_4x^4 \tag{4}$$

where y is the estimated response based on the fourth order equation, a_0, a_1, a_2, a_3, a_4 are the model parameters to be estimated using experimental data, and x (i.e. x_1, x_2, x_3, x_4) is the coded levels of the independent variables.

$$a_0 + a_1x + a_2x^2 + a_3x^3 + a_4x^4 = \left[(Ax+B)^2 + Ax + C\right]\left[(Ax+B)^2 + D\right] + E \tag{5}$$

where

$$A \equiv (a_4)^{1/4} \tag{6}$$

$$B \equiv \frac{a_s - A^3}{4A^3} \tag{7}$$

$$D \equiv 3B^2 + 8B^3 + \frac{a_1A - 2\ a_2B}{A^2} \tag{8}$$

$$C \equiv \frac{a_2}{A^2} - 2B - 6B^2 - D \tag{9}$$

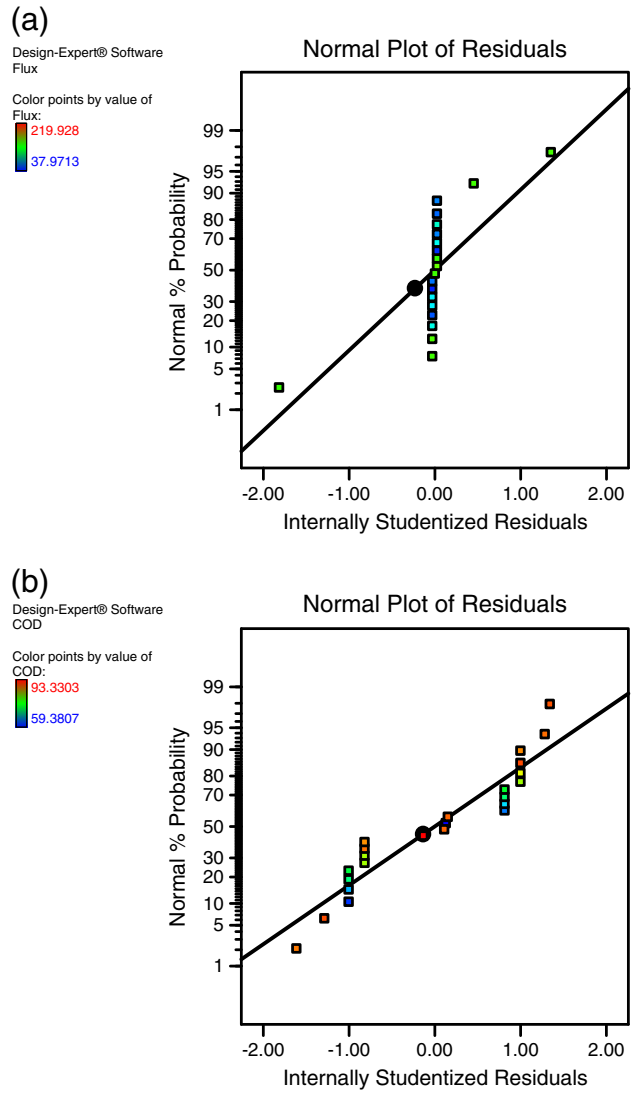

Fig. 4. Normal probability plot of residual for (a) flux and (b) COD removal.

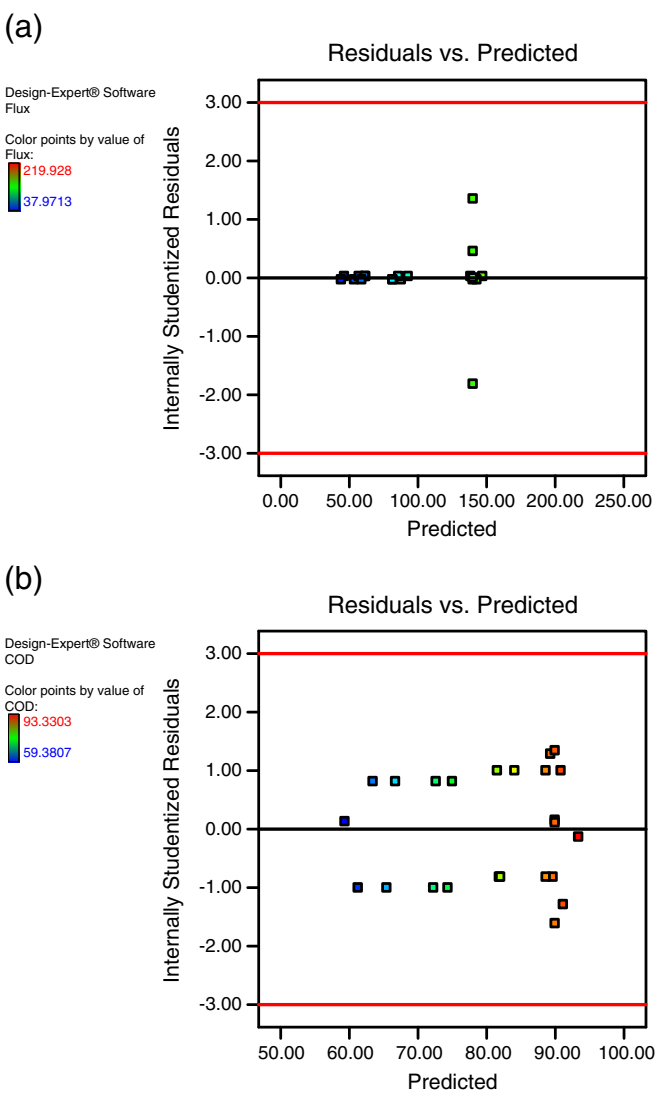

Fig. 5. Plot of residual against predicted response (a) flux and (b) COD removal.

$$E \equiv a_o - B^4 - B^2(C + D) - CD. \quad (10)$$

To facilitate the determination of constants and exponents, this mathematical model needs to be linearized by performing a logarithmic transformation, which can be written as:

$$\hat{y} = y - \varepsilon$$
$$\hat{y} = a_0x_0 + a_1x_1 + a_2x_2 + a_3x_3 + a_4x_4 + a_{11}x_1^2 + a_{22}x_2^2 + a_{33}x_3^2 + a_{44}x_4^2 + \cdots + a_{12}x_1x_2 + a_{13}x_1x_3 + a_{14}x_1x_4 + a_{23}x_2x_3 + a_{24}x_2x_4 + a_{34}x_3x_4 + \ldots + a_{123}x_1x_2x_3 + a_{124}x_1x_2x_4 + a_{134}x_1x_3x_4 + a_{234}x_2x_3x_4 + a_{1234}x_1x_2x_3x_4 \quad (11)$$

where y is the logarithmic value of the experimental tool life, $\hat{y}$ is the logarithmic value of the predictive (estimated) tool life, $x_0 = 1$ (a dummy variable), x_1, x_2 and x_3 are the coded value (logarithmic transformation), ε is the logarithmic transformation of experimental error ε' and a_0, a_1, a_2, a_3 and a_4 are the model parameters to be estimated using the experimental data.

Validity of the selected model used for optimizing the process parameters has to be tested using ANOVA.

All these coefficient variables are analyzed by multiple regression analysis and response contour plot is generated using the software Design-Expert.

In general, primary objective of RSM is to optimize the response (Y) based on the factors investigated [32]. The design expert software was used to develop the experimental plan and optimize the regression equation (Eq. (11)). The statistical significance of the second order model equation was determined by performing Fisher's statistical test for analysis of variance (ANOVA). In particular a good model must be significant based on F-value and P-value as opposed to the lack of fit (insignificant). Moreover the proportion of variance exhibited by the multiple coefficient of determination R^2 should be close to 1 as this would demonstrate better correlation between the experiment and the predicted values [33].

3. Results and discussion

3.1. Model fitting and statistical analysis

The second-order polynomial regression model containing 4 linear, 4 quadratic, and 6 interaction terms plus 1 block term was employed by using RSM. This model was found to be significant with $R^2 = 0.99$. Joglekar and May [34] also suggested that for a good fit of a model, R^2 should be at least 0.80. The R^2 for these response variables was higher than 0.80, indicating that the regression models

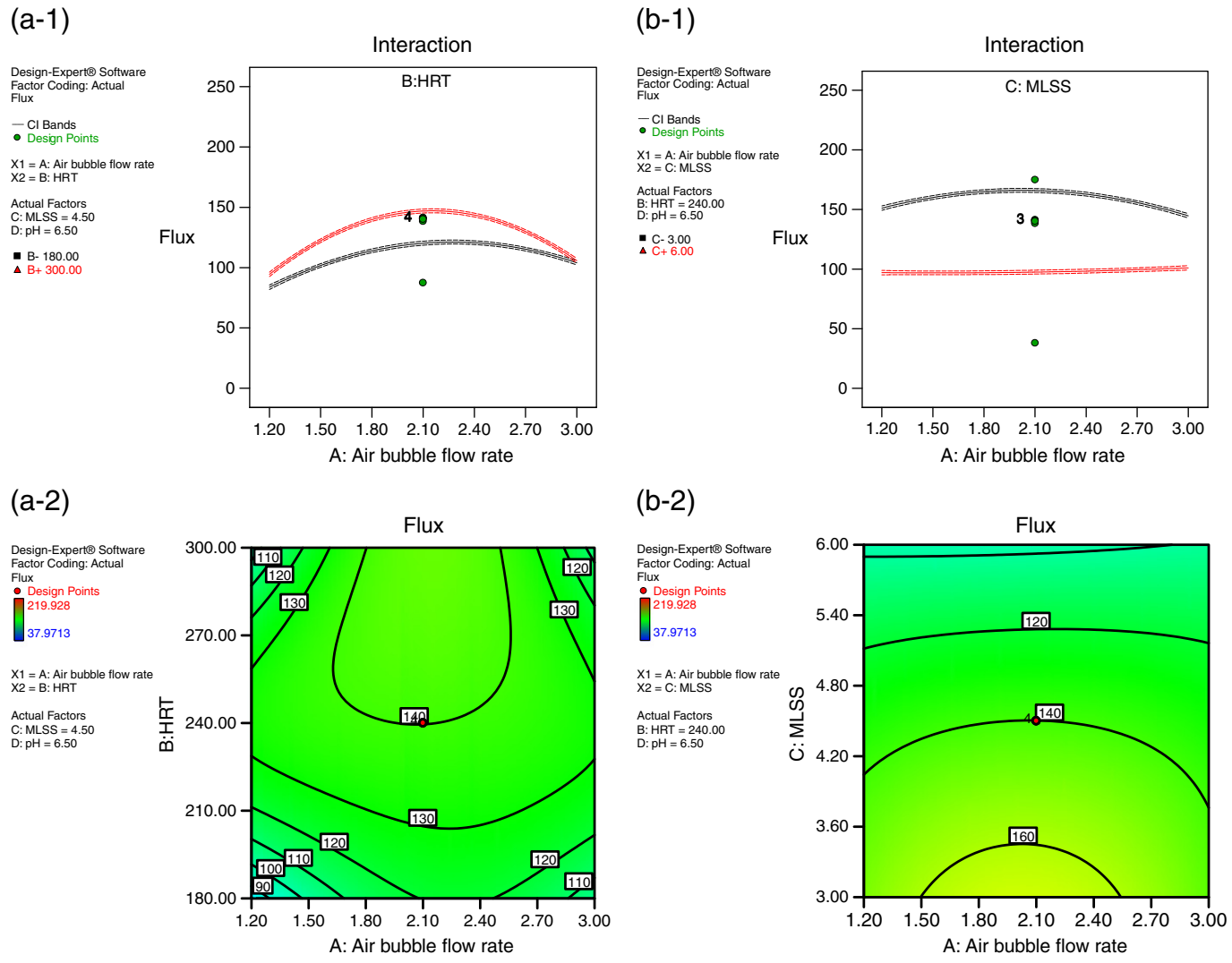

Fig. 6. Interaction graph (−1) and contour plot (−2) of flux from the model equation of effect the condition process: (a) ABFR-HRT, (b) ABFR-MLSS, (c) ABFR-pH, (d) HRT-MLSS, (e) HRT-pH, and (f) MLSS-pH.

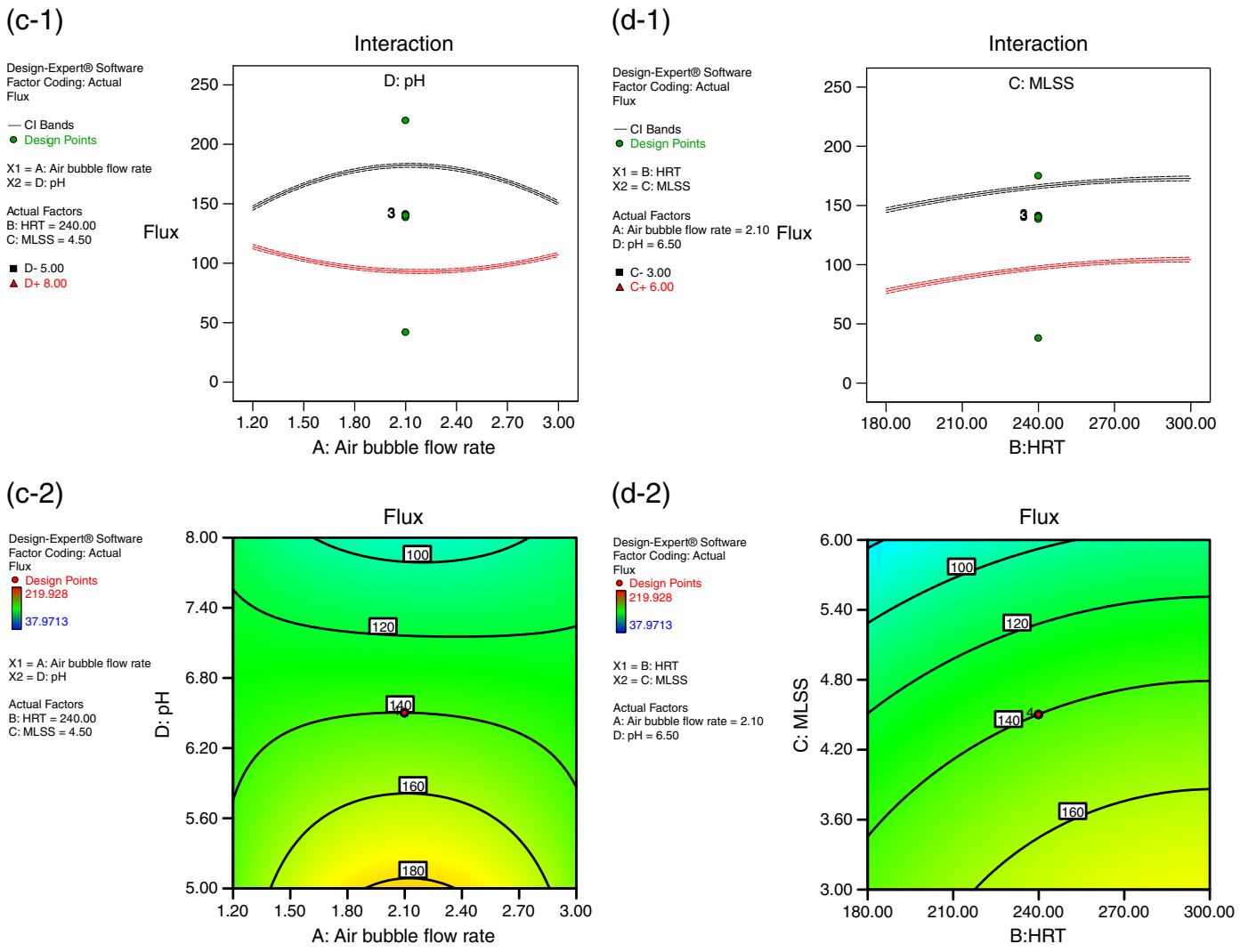

Fig. 6 (*continued*).

explained the reaction well. However, its lack of fit was significant ($P = 0.0229$), suggesting that this model did not accurately represent data in the experimental region. Therefore, it might be necessary to include higher order terms in the regression model. Since each factor had five levels, up to quartic terms could be included in the model [35].

In order to find a better model, variable selection techniques were used. The backward elimination procedure was employed to eradicate the insignificant terms and ANOVA results of this reduced quartic model. ANOVA is a statistical technique that subdivides the total variation in a set of data into component parts associated with the specific sources of variances for the purpose of testing hypotheses on the parameters of the models [36]. The ANOVA of these models have demonstrated that the model is highly significant as is evident from Tables 5 and 6 which tabulated the effects and interactions of ABFR, HRT, MLSS, and pH on flux and COD removal of filtered refinery wastewater.

A statistical testing using Fisher's statistical test for ANOVA was employed for the determination of significant variables where degree of significance was ranked based on the value of F-ratio. As the matter of fact the larger the magnitude of F-value and correspondingly the smaller the 'Prob>F' value, the more significant are the corresponding model and the individual coefficient [37–42]. It was observed from ANOVA analysis (Table 5) that the confidence level was greater than 80% ($P<0.05$) for flux response while F-value and P-value of the model were 2157.23 and 0.0001 respectively. This indicated that the estimated model fits the experimental data adequately. Furthermore the coefficient of determination R^2 of the model was reasonably close to 1 (0.9999), implying that about 99.9% of the variability in the data was explained by the model. It was further shown that the main effect of aeration flow rate (x_1), HRT (x_2), MLSS (x_3), and pH (x_4) and more level interactions of x_1x_2, x_1x_3, x_1x_4, x_2x_3, x_2x_4, x_1^2, x_2^2, x_3^2, x_4^2, $x_1x_2x_3$, $x_1x_2x_4$, $x_1x_3x_4$, $x_2x_3x_4$, $x_1^2x_2$, $x_1^2x_3$, $x_1^2x_4$, $x_1x_2^2$, and $x_1^2x_2^2$ were significant model terms (factors).

Table 6 shows the confidence level of ANOVA analysis of COD removal response which was greater than 80% ($P<0.05$) for COD response while F-value and P-value of the model were 508.75 and 0.0001 respectively. This indicated also that the estimated model fits the experimental data adequately. It was further shown that the main effect of aeration flow rate (x_1), HRT (x_2), MLSS (x_3), and pH (x_4) and more level interactions of x_1, x_2, x_3, x_4, x_1x_2, x_1x_3, x_1x_4, x_2x_3, x_2x_4, x_3x, x_1^2, x_2^2, x_3^2, x_4^2, $x_1x_2x_3$, $x_1x_2x_4$, $x_1x_3x_4$, $x_2x_3x_4$, $x_1^2x_2$, $x_1^2x_4$, $x_1x_2x_3x_4$, and $x_1^2x_2^2$ were significant model terms (factors).

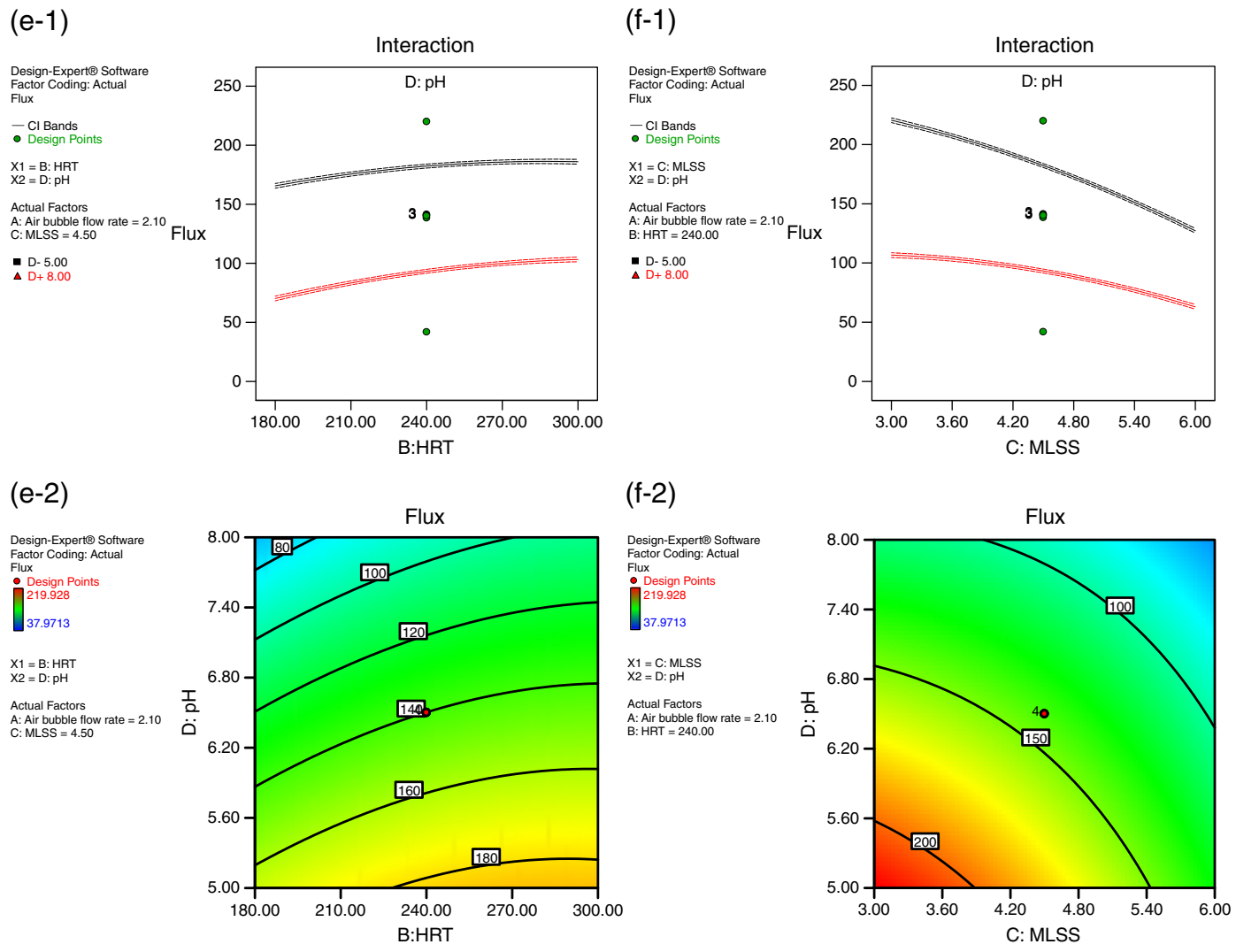

Fig. 6 (*continued*).

3.2. Response surface methodology approach for optimization of factors

Based on the RSM approach, the runs were conducted in CCD model-designed experiments to visualize the effects of independent factors on the response and the results along with the experimental conditions. According to the sequential model sum of squares, the model was selected based on the highest-order polynomials where the additional terms were significant. An empirical relationship between the response and the variables was expressed by the following fitting the equation fourth degree. The experimental results were evaluated and the approximating function of flux and COD removal, as shown in Eqs. (12)–(15), that were obtained in the final equation in terms of coded and actual factors are:

$$y_{1coded} = 140.10 - 0.63x_1 + 13.35x_2 - 34.24x_3 - 44.51x_4 - 2.23x_1x_2 + 2.61x_1x_3 - 2.71x_1x_4 - 0.015x_2x_3 + 3.16x_2x_4 + 12.41x_3x_4 - 8.91x_1^2 - 6.50x_2^2 - 8.41x_3^2 - 2.30x_4^2 - 0.85x_1x_2x_3 - 0.77x_1x_2x_4 - 5.18x_1x_3x_4 - 1.43x_2x_3x_4 - 10.26x_1^2x_2 + 9.79x_1^2x_3 + 25.61x_1^2x_4 + 8.54x_1x_2^2 - 28.39x_1^2x_2^2 \quad (12)$$

where the measured $y_{1actual}$ is defined as the flux of the permeate solution and x_1, x_2, x_3 and x_4 represent ABFR, HRT, MLSS, and pH, in terms of coded factor.

$$y_{1actual} = -2744.32 + 2977.41x_1 + 22.75x_2 - 50.20x_3 + 7.17x_4 - 19.94x_1x2 - 12.77x_1x_3 - 76.77x_1x_4 + 0.09x_2x_3 + 0.01x_2x_4 + 13.43x_3x_4 - 693.52x_1^2 \neg 0.05x_2^2 \neg 3.74x_3^2 \neg 1.02x_4^2 - 0.01x_1x_2x_3 - 0.009x_1x_2x_4 - 2.55x_1x_3x_4 - 0.01x_2x_3x_4 + 4.46x_1^2x_2 + 8.05x_1^2x_3 + 21.08x12x4 + 0.04x_1x_2^2 - 0.009x_1^2x_2^2 \quad (13)$$

where the measured $y_{1actual}$ is defined as the flux of the permeate solution and x_1, x_2, x_3 and x_4 represent ABFR, HRT, MLSS, and pH, in terms of actual factor.

$$y_{2coded} = 89.45 + 0.46x_1 + 0.79x_2 + 8.51x_3 + 0.28x_4 + 0.034x_1x_2 - 0.095x_1x_3 - 0.19x_1x_4 - 0.77x_2x_3 - 0.56x_2x_4 - 0.57x_3x_4 + 0.067x_1^2 - 0.46x_2^2 - 3.40x_3^2 - 2.96x_4^2 + 0.11x_1x_2x_3 0.15x_1x_2x_4 + 0.11x_1x_3x_4 - 0.18x_2x_3x_4 - 0.074x_1^2x_2 + 3.82x_1^2x_4 - 0.29x_1x_2x_3x_4 - 5.81x_1^2x_2^2 \quad (14)$$

where the measured y_2 is defined as the COD rejection in the permeate solution and x_1, x_2, x_3 and x_4 represent ABFR, HRT, MLSS, and pH, in terms of coded factor.

$$y_{2actual} = -208.48050 + 108.48x_1 + 0.23x_2 + 34.13x_3 + 43.11x_4 - 0.06x_1x_2 - 4.54x_1x_3 - 15.79x_1x_4 - 0.04x_2x_3 - 0.02x_2x_4 - 1.26x_3x_4 - 25.06x_1^2 - 9.06E-005x_2^2 - 1.93x_3^2 - 1.73x_4^2 + 0.02x_1x_2x_3 + 0.009x_1x_2x_4 + 0.64x_1x_3x_4 + 0.004x_2x_3x_4 + 0.03x_1^2x_2 + 3.15x_1^2x_4 - 0.002x_1x_2x_3x_4 - 6.76E-005x_1^2x_2^2 \quad (15)$$

where the measured y_2 is defined as the CODrejection in the permeate solution and x_1, x_2, x_3 and x_4 represent ABFR, HRT, MLSS, and pH, in terms of actual factor.

The above empirical model equations are mathematical correlation model that can be employed to predict and optimize the flux and COD removal within the range of variable factors of this experiment. Analysis on normal probability plot of the residual (Fig. 4) depicted nearly a straight line residual distribution, which denoting errors are evenly distributed and therefore support adequacy of the least-square fit. The results illustrated in Fig. 5 revealed that the models proposed are distinctively adequate and reasonably free from any violation of the independence or constant variance assumption, as studentized residuals are equally tabulated within red line of the x-axis.

3.3. Effects of interactive factors

The experimental design model was used to evaluate the effect and interaction between four process variables on submerged ultrafiltration process. The effect of process variables on flux and COD removal was analyzed using simulated interaction analysis graph and contour plot according to the backward quartic model (Figs. 6 and 7). Each plot represents the effect of two factors at their studied range with the other factors maintained at its zero level. The significance of interactions between factors on the flux can be best considered using interaction analysis graph in Fig. 6. Meanwhile, the shapes of the contour plots indicate the nature and extent of the interactions. Prominent interactions are shown by the elliptical nature of the contour plots, while less prominent or negligible interactions would otherwise be shown by the circular nature of the contour plots. The color degradation from blue to red was also illustrated as the higher value of responses.

It has been observed from Fig. 6(a-1) that the interaction effect between ABFR and HRT demonstrated a remarkable improvement in flux as ABFR increased from 1.2 mL/min to 2.1 mL/min and then decreased with further increased ABFR. It suggested that this variable significantly affects the flux. The enhancement brought by increasing flux appears to be greater at higher HRT condition (HRT of 300 min). In the interaction between ABFR and HRT on flux (Fig. 6(a-2)) at MLSS and pH of 4.50 g/L and 6.50, respectively, the flux peaked at approximately 145.37 L/m^2 h when the air bubble flow rate is 2.25 mL/min and HRT is 276.93 min. In addition, the change of flux was also analyzed as a function of all process variables studied. It should be noted that the similar trend occured in the change of ABFR. The flux value was found maximum at approximately zero coded level factor (0). It is worth to note that increase in flux at low MLSS and pH. This indicated that the greater ABFR led to a higher steady flux. This could be explained by the change of Reynold's number (*Re*). Re is defined as follows:

$$\mathrm{Re} = \frac{\rho \upsilon d}{\mu} \tag{16}$$

where ρ is the density of the liquid, υ the velocity of the liquid, d the distance in axial of membrane reservoir and μ is the viscosity of the liquid.

Therefore, the greater ABFR resulted in a larger Re. Theoretically, turbulent flow is defined as if the Re exceeds 4000. The turbulent flow, which weakened the effect of concentration polarization [43], occured as ABFR increased to 2.25 mL/min. Although high ABFR could enhance the flux, forceful turbulent is not recommended in UF membrane process. Ueda et al. [44] observed an optimum aeration rate beyond which a further increase has no effect on fouling supression. The turbulent flow may consume TMP of the system, causing weaker hydraulic and attachability factors which lead to the decline of the permeate flux.

The effect of pH on the membrane filtration is showed in Fig. 6(c, e, and f). The permeate flux was highly dependent on the pH of the feed solution. The flux increased sharply at low pH (pH of 5.00). Based on the contour plots (Fig. 6(e-2, f-2)), it can observed that flux increased with increasing HRT but decreased in further greater MLSS concentration. Fig. 6(d-1, d-2) shows the effect of MLSS and HRT on flux values, whereas the flux increased with increasing HRT at low MLSS concentration (MLSS of 3.00 g/L). A highest peak at approximately HRT of 273 min and MLSS of 3.00 g/L was observed in the resulted flux contour plot. The permeate flux under various pH values was affected not only by the characteristics of membrane but also by the properties of the solute (droplet). The size and zeta potential of the emulsion droplets in refinery wastewater indicated that obvious variation existed in the average size of droplets under various pH values [45]. The coagulation of emulsion did not occur under stable condition (i.e. pH 4–6) as the zeta potential of emulsion droplet was low in absolute value. While the emulsion droplets had the higher negative charge due to the presence of the surfactant (sodium dodecyl allyl sulfosuccinate). Therefore, the electrostatic affinity accelerates fouling formation since the droplets adsorb onto the membrane surface and penetrate into the membrane pores, lowering the steady permeate flux at pH >6. The declined flux seen at pH 8 was caused by irreversible foulant deposition on the upper surface of the membrane at higher pH, although the ABFR increased which was caused by higher turbulence flow. The increase of air bubble flow rate to 3.0 mL/min tends to increase the polarization resistance to higher values, but it often seen that there exists a critical aeration rate below which severe fouling occurs. Above this air bubble flow rate, there is a low improvement in fouling performance [46]. A higher shear rate due to extensive aeration can also have detrimental effects, as it increases the shear-induced diffusion and inertial lift forces for the large particles and causes small particle, which can induce severe pore blocking and irreversible gel formation to become the major foulants. Additionally, bubbles might be trapped in gas pockets between groups of fibers, minimizing effective membrane surface area.

Effects of ABFR, MLSS, HRT and pH on COD removal have been illustrated in Fig. 7. Highest peak was observed at ABFR of 2.25 mL/min and MLSS concentration of 4.5 g/L (Fig 7(a-2)). This value was achieved because the increased ABFR can lead to more sufficient supply of dissolved oxygen, which has a positive effect on the removal of COD because the oxygen is needed by aerobic microorganisms as the electronic acceptor. Meanwhile, the ABFR in membrane reservoir must be carefully controlled to maintain adequate expansion and liquid mass transfer while minimizing shear effect.

The similar patterns are also found by the effect of MLSS concentration and HRT, as shown in Fig. 7(b-1, b-2). COD removal increased slightly with increasing HRT at higher MLSS concentration. This indicated that the lower MLSS concentration (3.00 g/L), the microbial metabolism and COD removal were quite low. After adding the MLSS concentration to 6.00 g/L, the sludge increased and COD removal also increased with increasing of HRT. For further increasing HRT, the effluent COD increased slightly, but the operating charges would also increase accordingly. It was verified that good organic matter removal was achieved in the process especially considering the characteristic of the wastewater and the HRT. Taking into consideration the initial capital investment and the operating charges, HRT of 276.93 min was resulted from mathematical calculations using desirability function approach as the optimum value. Fig. 7(c-1, c-2, d-1, d-2) shows that pH exerts a remarkable influence on biological removal of COD. As can been seen in Fig. 7(c-1, c-2), the increase of pH values with increasing HRT resulted the similar results ofCOD removal, whereas the COD removal was remained at the range of 87–90%. The results of one-way ANOVA indicated that the average COD removal efficiencies had no significant difference under different pH conditions ($p > 0.05$).

3.4. Optimization of influencing factors

The main objective of the optimization is to determine the optimum values of factors for flux and COD removal efficiencies from the models obtained from the experiment. In this paper, optimum conditions are often calculated in the presence of some constraints in order to ensure them to be more realistic. Furthermore, the model used in the optimization study is an empirical basis, high and low levels of the process parameters in the experimental design are considered, inevitably, as explicit constraints, in order to avoid extrapolation.

Thus, the optimization problem is defined as:

$$Y \text{ is maximum} \tag{17}$$

and the constraints on the parameters X_i:

$$-1 < X_i < +1, \quad i = 1, 2, 3. \tag{18}$$

The optimization problem given in Eq. (17) is solved using constrained optimization program supplied in theRSM optimization toolbox. The optimized reaction conditions are sorted by order of descending desirability. Desirability is an objective function that reflects the desirable ranges for each factor and is defined as the geometric means of all transformed factors. The response results with standard deviation and desirability of 0.981 are listed in Table 7.

3.5. Verification of the results

To confirm the model adequacy for predicting maximum response results, four factors experiments using this optimum operation conditions were performed in Table 7.

These experiments yielded an average maximum response results that are listed in Table 5. The obtained actual values and its associated predicted values from the experiments were compared for further residual and percentage error analysis. The percentage error between actual and predicted value of the responses was calculated based on Eq. (19):

$$\%\,\text{Error} = \frac{\text{Residual}}{\text{Actual value}} \times 100\% \tag{19}$$

where residual can be determined from the difference between actual value and predicted value; actual value is the experimental value of this study.

Results in Table 8 have shown that the percentage errors implied by the developed empirical model are considerably accurate for all

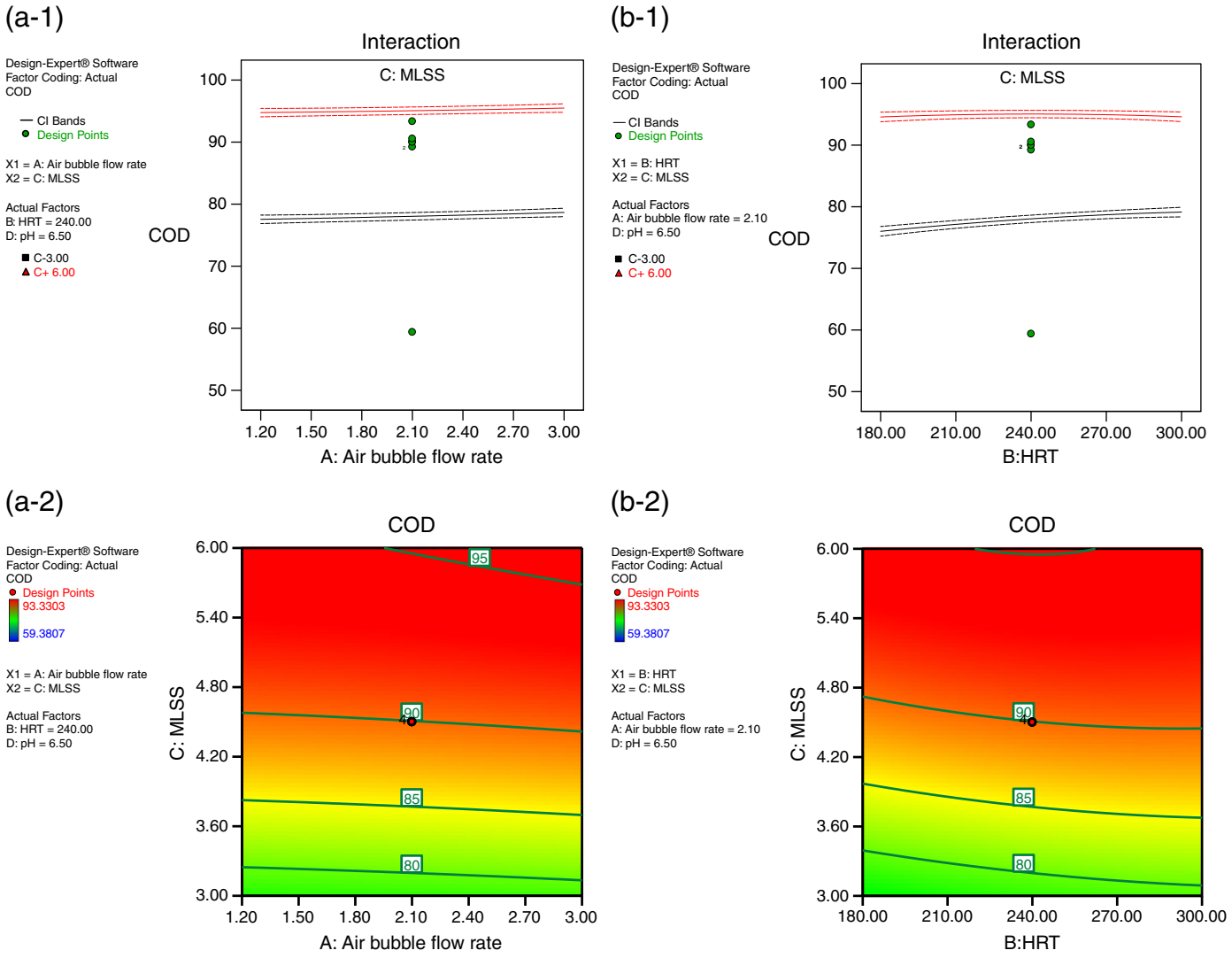

Fig. 7. Interaction graph (−1) and contour plot (−2) of COD removal from the model equation of effect the condition process: (a) ABFR-MLSS, (b) HRT-MLSS, (c) HRT-pH, and (d) MLSS-pH.

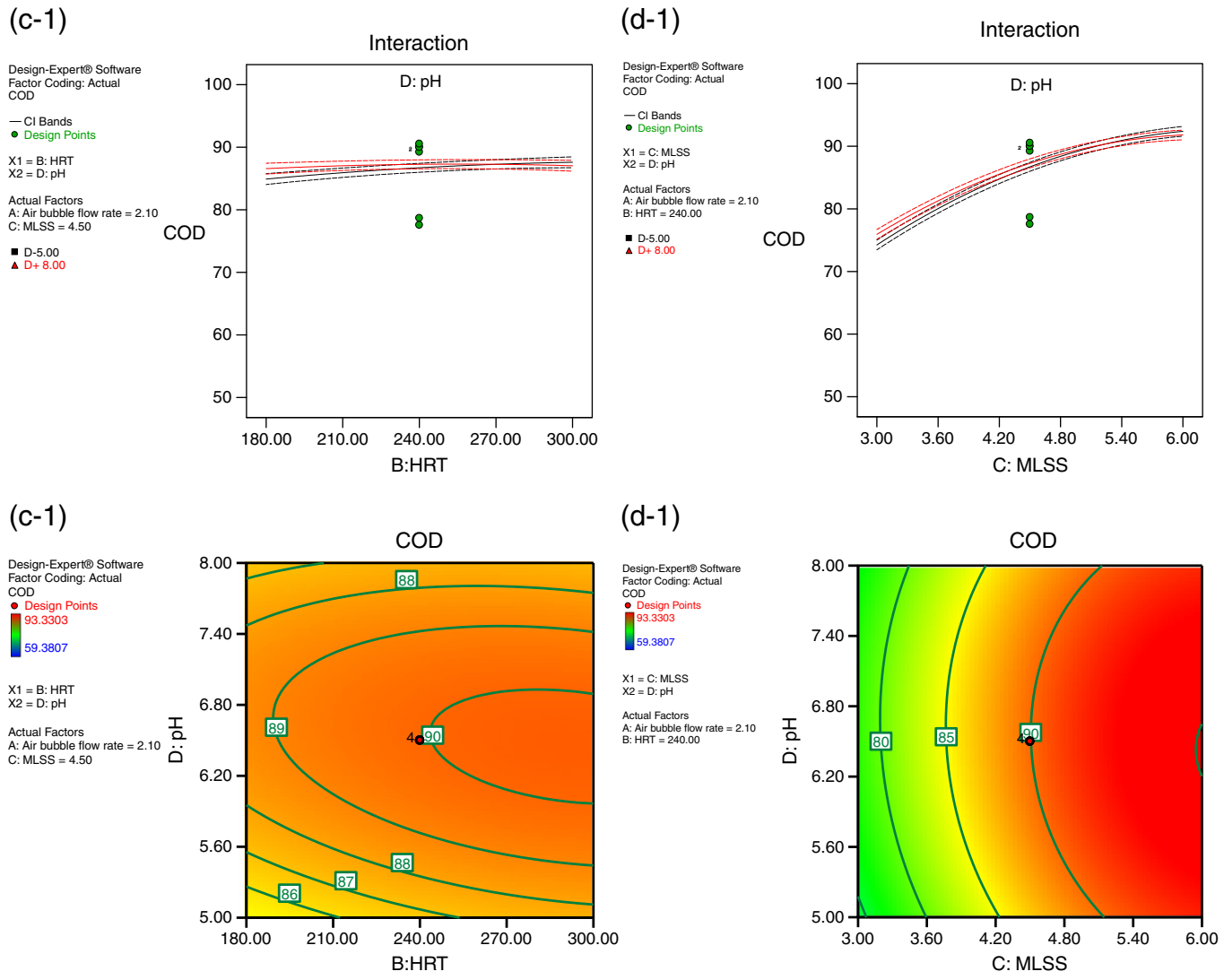

Fig. 7 (*continued*).

responses. The percentage error between the actual and predicted values was well within the value of 5%, suggesting that the model adequacy is reasonable within the 95% of prediction interval [47]. The good agreement between the predicted and experimental results verified the validity of the model and reflected the existence of an optimal point. By this means further analysis with regards to ideal operational process for optimal membrane performance would be based on this developed model. The results derived from this study indicated also that the RSM is a powerful tool for optimizing the individual factors.

4. Conclusions

A full factorial design and central composite design of response surface methodology can be used to determine the significant variables and optimum condition for submerged ultrafiltration of refinery wastewater with respect to flux and COD removal. Experimental results showed that a submerged ultrafiltration process using modified PVDF membranes has a great potential for refinery produced wastewater treatment. The quartic equation developed in this study shows the presence of a high correlation between observed and predicated values.

Table 7
Optimum value of the factors (process parameters) for maximum response results.

Factors	Optimum value	S.D.
Y_1 (flux, L/m^2 h)	145.37	1.08
Y_2 (COD removal efficiency, %)	90.28	0.51
X_1 (aeration flow rate, mL/min)	2.25	–
X_2 (HRT, min)	276.93	–
X_3 (MLSS, g/L)	4.50	–
X_4 (pH)	6.50	–

Table 8
Predicted and experimental value for the responses at optimum condition.

	Responses	
	Flux	COD removal efficiency, %
Predicted	145.37	90.28
Experimental	144.59	90.05
Residual	0.78	0.23
% error	0.54	0.26

Interestingly, 2-dimension response surface plots can be a good driven approach for visualizing the parameter interaction. The optimum factor conditions that were satisfied at ABFR of 2.25 mL/min, HRT of 276.93 min, MLSS concentration of 4.50 g/L, and pH of 6.50 resulted to flux of 145.37 L/m^2 h and COD removal of 90.28%.

The statistical approach has been testified to be a powerful tool in studying submerged ultrafiltration process. Further pilot scale studies are required and detailed study is needed to explore the refinery wastewater filtration mechanism.

Acknowledgments

The authors gratefully acknowledged the Research Management Center, Universiti Teknologi Malaysia, for supporting this research through Research University Grant, Vot. No. Q.J130000.7109.01H64.

References

[1] L.E. Fratila-Apachitei, M.D. Kennedy, J.D. Linton, I. Blume, J.C. Schippers, Influence of membrane morphology on the flux decline during dead-end ultrafiltration of refinery and petrochemical wastewater, J. Membr. Sci. 182 (2001) 151–159.
[2] W. Lee, S. Kang, H. Shin, Sludge characteristics and their distribution to microfiltration in submerged membrane bioreactors, J. Membr. Sci. 216 (2003) 217–227.
[3] R. Rautenbach, R. Albrecht, Membrane Processes, John Wiley and Sons, New York, 1989.
[4] http://www.mkma.org/EnvironmentalRegulation2009.htm., Notice Board: Environmental Quality (Industrial Effluent) Regulation 2009.
[5] D. Jeison, J.B. van Lier, Cake layer formation in anaerobic submerged membrane bioreactors (AnSMBR) for wastewater treatment, J. Membr. Sci. 284 (2006) 227–236.
[6] F. Wicaksana, A.G. Fane, V. Chen, Fibre movement induced by bubbling using submerged hollow fibre membranes, J. Membr. Sci. 271 (2006) 186–195.
[7] P. Le-Clech, B. Jefferson, S.J. Judd, Impact of aeration, solid concentration and membrane characteristics on the hydraulic performance of a membrane bioreactor, J. Membr. Sci. 218 (2003) 117–129.
[8] K.J. Howe, M.M. Clark, Fouling of microfiltration and ultrafiltration membranes by natural waters, Environ. Sci. Technol. 36 (16) (2002) 3571–3576.
[9] A.F. Viero, T.M. de Melo, A.P.R. Torres, N.R. Ferreira, G.L. Sant'Anna Jr., C.P. Borges, V.M.J. Santiago, The effects of long-term feeding of high organic loading in a submerged membrane bioreactor treating oil refinery wastewater, J. Membr. Sci. 319 (2008) 223–230.
[10] A.W. Zularisam, A.F. Ismail, R. Salim, Mimi Sakinah, H. Ozaki, The effects of natural organic matter (NOM) fractions on fouling characteristics and flux recovery of ultrafiltration membranes, Desalination 212 (1–3) (2007) 191–208.
[11] Z. Yuan, X.D. Li, Porous PVDF/TPU blends asymmetric hollow fiber membranes prepared with the use of hydrophilic additive PVP (K30), Desalination 223 (2008) 438–447.
[12] P.Z. Çulfaz, M. Wessling, R.G.H. Lammertink, Fouling behavior of microstructured hollow fiber membranes in submerged and aerated filtrations, Water Res. 45 (2011) 1865–1871.
[13] G. Guglielmi, D. Chiarani, S.J. Judd, G. Andreottola, Flux criticality and sustainability in a hollow fibre submerged membrane bioreactor for municipal wastewater treatment, J. Membr. Sci. 289 (2007) 241–248.
[14] L. Xianling, W. Jianping, Y. Qing, Z. Xuemin, The pilot study for oil refinery wastewater treatment using a gas–liquid–solid three phase flow airlift-bioreactor, Biochem. Eng. J. 27 (2005) 40–44.
[15] A.W. Zularisam, A.F. Ismail, R. Salim, Behaviour of natural organic matter in membrane filtration for surface water treatment: a-review, Desalination 194 (2006) 211–231.
[16] J. Saien, H. Nejati, Enhanced photocatalytic degradation of pollutants in petroleum refinery wastewater under mild conditions, J. Hazard. Mat. 148 (2007) 491–495.
[17] M.L. Hami, M.A. Al-Hasyimi, M.M. Al-Doori, Effect of activated carbon of BOD and COD removal in a dissolved air flotation unit treating refinery wastewater, Desalination 216 (2007) 116–122.
[18] A.W. Zularisam, A.F. Ismail, M.R. Salim, Mimi Sakinah, O. Hiroaki, Fabrication, fouling and foulant analyses of asymmetric polysulfone (PSf) ultrafiltration membrane fouled with natural organic matter (NOM) source waters, J. Membr. Sci. 229 (2007) 97–113.
[19] W.J. Lau, A.F. Ismail, Application of response surface methodology in PES/SPEEK blend NF membrane for dyeing solution treatment, Membr. Water Treat. 1 (2010) 49–60.
[20] J. Fu, Y. Zhao, Q. Wu, Optimising photoelectrocatalytic oxidation of fulvic acid using response surface methodology, J. Hazard. Mat. 144 (2007) 499–505.
[21] E.M. Silva, H. Rogez, Y. Larondelle, Optimization of extraction of phenolics from Inga edulis leaves using response surface methodology, Sep. Purif. Technol. 55 (2007) 381–387.
[22] G. Güven, A. Perendeci, A. Tanyolaç, Electrochemical treatment of deproteinated whey wastewater and optimization of treatment conditions with response surface methodology, J. Hazard. Mat. 157 (2008) 69–78.
[23] D. Jeison, J.B. van Lier, Cake layer formation in anaerobic submerged membrane bioreactors (AnSMBR) for wastewater treatment, J. Membr. Sci. 284 (2006) 227–236.
[24] D.P. Saroj, G. Guglielmi, D. Chiarani, G. Andreottola, Subcritical fouling behavior modelling of membrane bioreactors for municipal wastewater treatment: the prediction of the time to reach critical operating condition, Desalination 231 (2008) 175–181.
[25] D.M. Wardrop, R.H. Myers, Some responce surface designs for finding optimal conditions, J. Stat. Plan. Infer. 25 (1990) 7–28.
[26] R. Myers, D.C. Montgomery, Response Surface Methodology, John Wiley, New York, USA, 2002.
[27] E. Yuliwati, A.F. Ismail, Effect of additives concentration on the surface properties and performance of PVDF ultrafiltration membranes for refinery wastewater treatment, Desalination 273 (2011) 226–234.
[28] E. Yuliwati, A.F. Ismail, T. Matsuura, M.A. Kassim, M.S. Abdullah, Effect of modified PVDF hollow fiber submerged ultrafiltration membrane for refinery wastewater treatment, Desalination, in press.
[29] S.R. Smith, T. Taha, Z.F. Cui, Enhancing hollow fiber ultrafiltration using slug-low — a hydrodynamic study, Desalination 146 (2002) 69–74.
[30] J. Busch, A. Cruse, W. Marquardt, Modelling submerged hollow-fiber filtration for wastewater treatment, J. Membr. Sci. 288 (2007) 94–111.
[31] A.I. Khuri, J.A. Cornell, Response Surfaces: Designs and Analysis, Marcel Dekker, ASQA Quality Press, New York, 1996.
[32] E.L. Soo, A.B. Salieh, M. Basri, Response surface methodological study on lipase-catalyzed synthesis of amino acid surfactants, Process. Biochem. 39 (2004) 1511–1518.
[33] Y.X. Wang, Z.X. Lu, Optimization of processing parameters for the mycellial growth and extracellular polysaccharide production by Boletus spp. ACCC 50328, Process. Biochem. 40 (2005) 6549–6559.
[34] A.M. Joglekar, A.T. May, Product excellence through design of experiments, Cereal Foods World 32 (1987) 857–868.
[35] Design-Expert® Software Version 6 User's Guide, 2001.
[36] P. Rana-Madaria, M. Nagarajan, C. Rajapagol, B.S. Garg, Removal of chromium from aqueous solutions by treatment with carbon aerogel electrodes using response surface methodology, Ind. Eng. Chem. Res. 44 (2005) 6549–6559.
[37] L.C. Chen, C.M. Huang, M.C. Hsiao, F.R. Tsai, Mixture design optimization of the composition of S, C, SnO_2-codoped TiO_2 for degradation of phenol under visible light, Chem. Eng. J. 165 (2010) 482–489.
[38] I. Khouni, B. Marrot, R.B. Amar, Decolourization of the reconstituted dye bath effluent by commercial laccase treatment: optimization through response surface methodology, Chem. Eng. J. 156 (2010) 121–133.
[39] Z.F. Cui, S. Chang, A.G. Fane, The use of gas bubbling to enhance membrane processes, J. Membr. Sci. 221 (2003) 1–35.
[40] T. Ueda, K. Hata, Treatment of domestic sewage from rural settlements by a membrane bioreactor, Water Sci. Technol. 34 (1996) 186–196.
[41] D.C. Montgomery, Design and Analysis of Experiments, 4th ed. John Wiley & Sons, USA, 1996.
[42] R.H. Myers, D.C. Montgomery, Response Surface Methodology: Process and Product Optimization using Designed Experiments, 2nd ed. John Wiley & Sons, USA, 2002.
[43] R.J. Baker, A.G. Fane, C.J.D. Fell, B.H. Yoo, Factors affecting flux in crossflow filtration, Desalination 53 (1985) 81–93.
[44] T. Ueda, K. Hata, Y. Kikuoka, O. Seino, Effects of aeration on suction pressure in a submerged membrane bioreactor, Water Res. 31 (1997) 489–494.
[45] D.E. Tambe, M.M. Sharma, Factors controlling the stability of colloid-stabilized emulsion, J. Colloid Interf. Sci. 157 (1993) 244–253.
[46] D.B. Mosqueda-Jimenez, R.M. Narbaitz, T. Matsuura, G. Chowdhury, G. Pleizier, J.P. Santerre, Influence of processing conditions on the properties of ultrafiltration membranes, J. Membr. Sci. 231 (2004) 209–224.
[47] A.W. Zularisam, A.F. Ismail, M.R. Salim, Sakinah Mimi, T. Matsuura, Application of coagulation–ultrafiltration hybrid process for drinking water treatment: optimization of operating conditions using experimental design, Sep. Purif. Technol. 65 (2009) 193–210.